Electronic Supplementary Material (ESI) for Nanoscale.

Supporting Information

Operando surface optical nanometrology reveals diazonium salts visible photografting mechanism

Baptiste Maillot, Madelyn Johnson, Jean-Frédéric Audibert, Fabien Miomandre, Vitor Brasiliense*

S1) Evolution of the grafted layer optical thickness

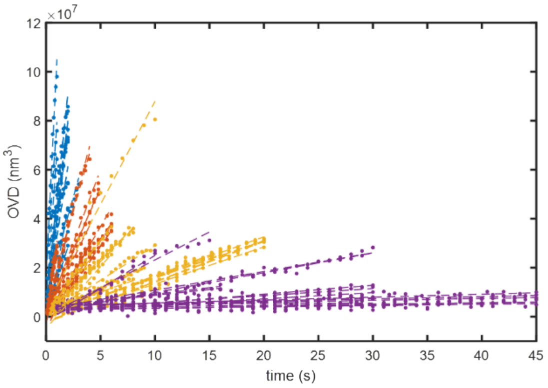

Figure S1. Evolution of the OVD as a function of time for several concentrations (0.625-20 mM and excitation power – corresponding to the same data shown in Figure 1). The colors indicate curves the power used (blue :200 µW, orange: 50 µW, yellow: 12.5 µW , purple: 3.12 µW).

S2) Evaluation of the diffusional limit for a disk grafting zone

Diffusive transport towards a disk shaped zone (defined as the laser waist on the surface), leads to a concentration profile described in cylindrical coordinates (r,z) as the solution to the following PDE:

$$\frac{\partial C(r,z,t)}{\partial t} = D\left[\frac{\partial^2 C(r,z,t)}{\partial r^2} + \frac{1}{r}\frac{\partial C(r,z,t)}{\partial r} + \frac{\partial^2 C(z,r,t}{\partial z^2}\right]$$

The diffusive limit is stablished when the reaction rate is much faster than diffusive transport, which leads to the following boundary conditions:

$C = C_{bulk}$ at t = 0, and at the limits $r \to \infty$ and $z \to \infty$

$C = 0$ at z = 0, r<r_0 , t>0

$\frac{\partial C}{\partial z} = 0$ at z = 0, r>r_0 t>0

The problem is strictly analogous to the determination of the steady state current at a disky microelectrode, and has been described in detail in [1]. The steady state flux of reactant is obtained from :

$$\varphi(t) = 4r_0 D\, C_{bulk}\, f\left(\frac{4Dt}{r_0^2}\right)(= i_{SS}/nF)$$

In which D is the grafting species diffusion coefficient, C_{bulk} its bulk concentration, r_0 the species sink region. Iss, n F are respectively the electrochemical steady state current, number of exchanged electrons per molecule and Faraday constant in the electrochemical analogue problem. $f(\tau)$ is a numerical term which depednds on the time since establshement of the flux, and that can be approximated for $\tau = 4Dt/r_0^2 > 1$ as: [1,2]

$$f(\tau) \cong 1 + 0.71835\tau^{-\frac{1}{2}} + 0.05626\tau^{-\frac{3}{2}} + 0.00646\tau^{-\frac{5}{2}} + \ \ldots$$

Which quickly converges to 1 (within 1%) after $\tau = 5$, or t = 5 ms ($D=10^{-9} m^2/s$, r_0 = 1µm). Therefore, taking $C_{bulk} =$ 5 mM, D = 10^{-9} m^2/s, and r_0 = 1 µm, a maximal expected flux of 2 × 10^{-14} mol/s is estimated, as stated in the main text.

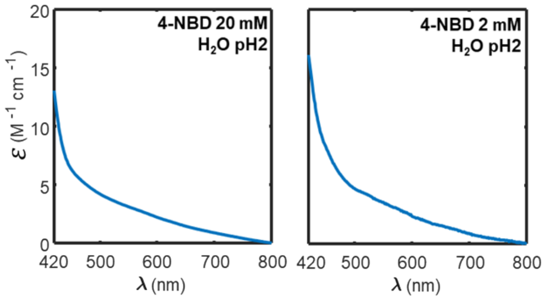

S3) UV-Vis Absorption Spectra

Figure S2. Comparison between the UV/Vis absorption spectra for 2 mM and 20 mM 4-NBD solutions (solvent : H_2O pH2, HCl), showing no evidence of complexation or π-π stacking.

S4) Grafting rate wavelength dependency for

Diazonium salt synthesis Following the classical diazotization procedure (detailled in the methods section), a 5 mM diazonium aqueous solution (pH2, HCl) was prepared from its aniline precursor (toluidine). The grafting rate was evaluated at different wavelengths using the same procedure as described for 4NBD in the main text. As it can be seen in the Figure S3, the presence of a small peak in the visible range anticipates the onset of the grafting reaction, which can be evaluated for wavelengths as high as 540 nm.

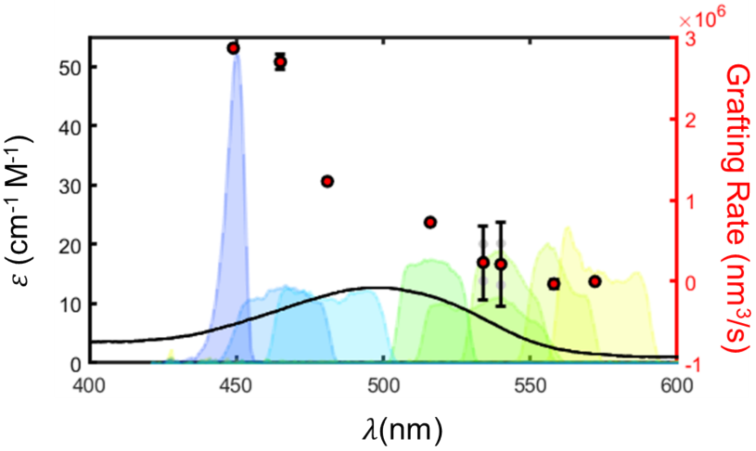

Figure S3. Action plot comparing the absorption spectra, and the grafting rate of p-toluidine-diazonium salt as a function of the excitation wavelength (5mM in pH2 HCl aqueous solvent . The background spectra represent the normalized exicitation spectra and error bars represent 3σ errors for the mean value.

S5) Expected propostionality between temperature and refractive index increase

We evaluate the expected ΔT leading to a Δn of 1 nm (SNR = 1) at $\lambda =$ 633 nm, using experimental dn/dT expresion described eq. 2 , valid for the range 270K to 350K:[3]

$$\frac{dn}{dT} = -B\left[1 - \exp\left(-\frac{T - T_0}{T_k}\right)\right]$$

Where B = 26.2 $\times$ 10^{-5} K^{-1} , T_0 = 2 °C and T_k = 48.5 °C, which leads to dn/dT = -(1.1 $\pm$ 0.3) $\times$ 10^{-4} K^{-1}. The expected refractive index change is thus evaluated, assuming that only region within an Rayleigh distance (estimated from the beam waist ω_0 as $L_R = \frac{\pi\omega_0^{0.5}}{\lambda}$) from the focal plane influences our measurement:

$$OPD = \Delta n \times L_R = \frac{dn}{dT} \times \Delta T \times L_R \Rightarrow \Delta T = OPD / \left(\frac{dn}{dT} \times L_R\right)$$

Therefore the minimal measurable OPD (corresponding to SNR =1), would be obtained for a ΔT of 1 $\pm$ 0.2 °C at room temperature, as illlustrated in Figure S4, leading to the estimation given in the main text.

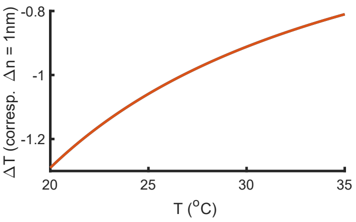

Figure S4. Temperature difference expected to lead to a phase difference of 1 nm.

S6) Degradation analysis in the presence of DMSO

In order to better understand the deactivation behavior observed in the presence of DMSO, we perform a series of bulk irradiation experiments, monitrored through the H^1 NMR spectra. The products were formed by directly illuminating the NMR tube with UV lamp (Hammamatsu LC8) at maximal power for 5 minutes. In Figure S5 we compare the H^1 NMR spectra before and after illumination in the presence and absence of d6-DMSO. The resulting spectra are recalibrated using residual DMSO as a reference at 2.3 ppm.

Before irradiation, the H1 NMR reveals, as spected a relatively simple feature, corresponding to the two characteristic doublets of 4-nitrobenzenediazonium (δ 8.44 and 8.55, J = 9.2Hz in d_6-DMSO/D_2O 1:1 mixture, δ 8.58 and 8.75, J = 9.2Hz in D_2O). Irradiation of the solution in deuterated water (Fig S5B), only leads to minor modification of the spectra, with the apparition of trace-level degradation product (δ 8.03 and 6.83, J = 9.2Hz). When the experiment is carried out in the presence of d_6-DMSO, several new peaks appear, which we attribute to three distinct products generated by a chain of reactions initiated by irradiation, as indicated in the figure. Considering the relatively simple medium, the radical species potentially present, and the structure of the signal, we *tentatively* assign the spectra as follows: (in blue) (i) p-substituted dinitro-azobenzene, resulting from the attack of a pristine diazonium ion by a radical the presence of azobenzene is also supported by its distinctive yellow color. (in orange) (ii) p d_5-DMSO-substituted nitrobenzene, resulting from interaction between nitrobenzene radical and d_5-DMSO radicals resulting from D-atom abstraction (iii) (in yellow) (iii) p-deuterated nitrobenzene, formed by abstraction of a D atom from d_6DMSO by a phenyl radical, in aggreement with the chemical shift observed for the ortho and meta protons of nitrobenzene (not shown).

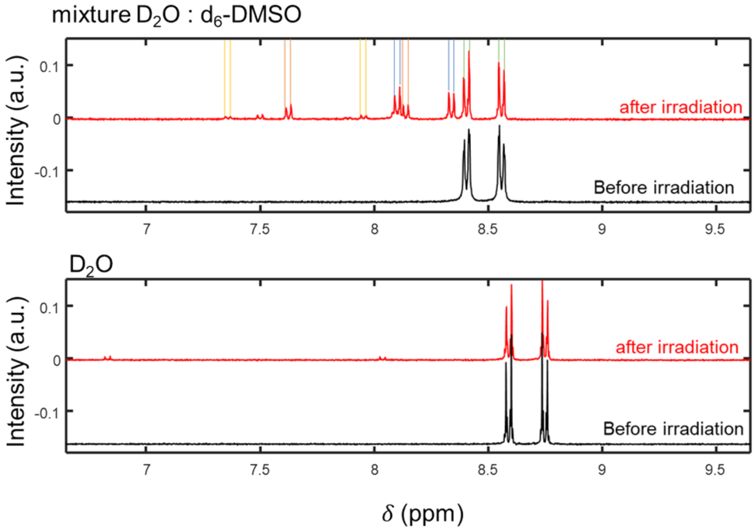

Figure S5. H1 NMR spectra of 4-NBD in different solvents, before and after irradiation, in either a 1:1 mixture of (A) D_2O:d_6-DMSO or (B) D_2O, putting in evidence the formation of several products when irradiation is carried out in the presence of DMSO.

References :

1 A. J. Bard and L. R. Faulkner, *Electrochemical Methods: Fundamentals and Applications, 2nd Edition*, Wiley Textbooks, 2000.

2 K. Aoki, K. Akimoto, K. Tokuda, H. Matsuda and J. Osteryoung, *Linear sweep voltammetry at very small stationary disk electrodes*, Elsevier Sequoia S.A, 1984, vol. 3.

3 X. Y. Wang, Z. S. Zhu, Y. K. Lu, G. Abbate, U. Bernini, E. Ragozzino and F. Somma, *The temperature dependence of the refractive index of water*, 1978, vol. 11.